DEVELOPMENT OF A REGIONAL-SCALE POLLEN EMISSION AND TRANSPORT MODELING FRAMEWORK FOR INVESTIGATING THE IMPACT OF CLIMATE CHANGE ON ALLERGIC AIRWAY DISEASE

Rui Zhang*, Serena H. Chung, Brian K. Lamb and Timothy M. VanReken
Laboratory for Atmospheric Research, WSU, Pullman, WA, USA

Tiffany Duhl and Alex Guenther
National Center for Atmospheric Research, Boulder, CO, USA

Muhammad T. Salam, Edward L. Avol and Frank D. Gilliland
University of Southern California, Los Angeles, CA, USA

James M. House and Richard C. Flagan
Department of Chemical Engineering, Caltech, Pasadena, CA, USA

Jeremy Avise
California Air Resource Board, Sacramento, CA, USA

1. INTRODUCTION

Exposure to respirable allergenic materials from ruptured pollen grains can stimulate the production of antibodies in human body and trigger allergic airway diseases (AAD), such as asthma, sinusitis and hay fever. The situation may become even more severe in the future due to intensive human activities that perturb the environment and land management practices, which will shift the pollen amount, pollen allergenicity, duration of pollen season and pollen spatial distributions. Hence, building a quantitative model to link airborne pollen levels, concentrations of respirable allergenic material and human allergenic response under current and projected future climate conditions is beneficial to access the health impacts of AAD and develop corresponding preventive actions. Logically, simulation the spatial-temporal variation of pollen occurrence stands the central role for this task.

In recently years, the idea to simulate regional pollen dispersal under the framework of sophisticated regional air-quality modeling system became popular. The advantage of this method is mainly two fold. First, it can be used in forecast mode to predict the pollen concentrations on a daily basis. Second, the predicted air pollutant concentrations are also important to allergy assessment. The adjuvant effects of pollution and pollen exposure on AAD can be evaluated under the same modeling framework.

A new pollen emission model from terrestrial, temperate vegetation has been developed and incorporated into the WRF/CMAQ regional air-quality modeling framework in this study. It is a regional pollen dispersion simulation platform with the flexibility to predict the temporal-spatial variations of different pollen species under current and future climate conditions. The model results can be linked with ADD clinical data to access and forecast pollen impact on target sensitive groups. Model evaluation has been carried out by simulating representative allergenic pollen species during the Mar-Jun 2010 flowering season over Southern California where the Children Health Study (CHS) campaign had collected pollen count as well as pollen sensitization data. The uncertainties of the emission and transport module of this modeling framework are also discussed through sensitivity studies.

2. METHODOLOGY

2.1 WRF-MEGAN-CMAQ modeling framework

The schematic flowchart depicting the regional air-quality modeling framework including pollen is given in Fig 1, with the core pollen-relevant modules highlighted in grey. The key meteorological variables for pollen dispersion, such as wind speed and direction, temperature, relative humidity (RH), radiation and dew point

**Corresponding author:* Rui Zhang, Department of Civil and Environmental Engineering, Washington State University, Pullman, WA, 99164-2910.
Tel: (+1)509-335 -4921; e-mail: mazhangr@gmail.com

temperature are predicted by NCAR's state-of-art mesoscale WRF Model. The NCAR Simulator of the Timing And Magnitude of Pollen Season (STAMPS) model, a module within bio-emission model MEGAN simulates the pollen production capacity and timing of pollen season and is driven by temperature and precipitation provided by WRF through the MCIP utility. The Models-3 CMAQ modeling system from US EPA is applied as the host model to simulate pollen transport.

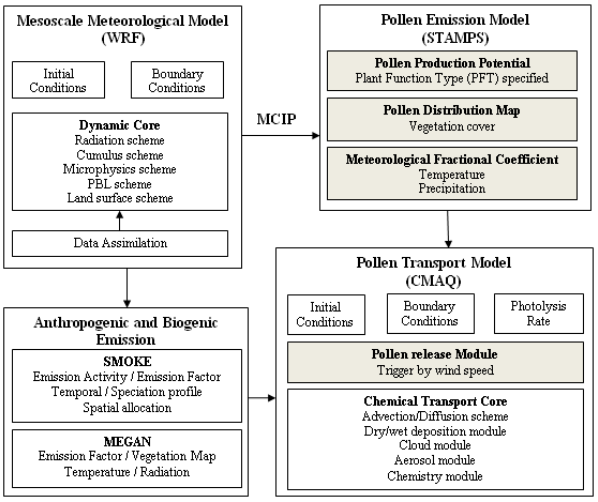

Fig 1. Flowchart of regional WRF-MEGAN-CMAQ air quality modeling framework with pollen emission and transport modeling highlighted

2.2 Simulation domains and model configurations

Two nesting domains with horizontal grid cell sizes of 12 km × 12 km (D1) and 4 km × 4 km (D2) with 105 × 95 (D1) and 126 × 93 (D2) cells were set up for the WRF and CMAQ models with domain coverage shown in Fig 2. The purpose of D1 is to minimize the impact of uncertain boundary conditions to the simulation results. The WRF version 3.2.1 meteorological simulations were driven by initial and boundary conditions from the North American Regional Reanalysis Results (NARR). Twenty-nine vertical layers were constructed from the ground to 50 mb with 11 vertical layers below 1 km. The physical option chose for the WRF simulation are YSU scheme for PBL simulation, Thompson scheme for microphysics, thermal diffusion methods for land-surface model and Monin-Obukhov profile for surface scheme. Analysis nudging was applied to the outer domain while observational nudging was applied to the inner domain using wind and temperature data that were obtained from the California Air Resources Board (CARB) from 46 meteorological stations throughout the region.

Model simulation was running during March-June 2010 where pollen counts and the fractional exhaled nitric oxide (FeNO) level for asthma sensitivity were measured within eight sites of the University of Southern California Children's Health Study (CHS) communities to probe the spatial variability in pollen exposures and heath impacts. Plus the long term pollen counts observations at Caltech campus, in total 9 sites daily mean pollen observation data are available for model comparison (see Fig 2).

Six pollen genera containing one or more important allergenic species that typically bloom during the selected simulation time (March-June) over southern California were included in the model: betula (birch tree), bromus (brome grass), juglans (walnut tree), morus (mulberry tree), olea (olive tree), and quercus (oak tree). The timing of pollen season for each genus is determined by comparing accumulated thermal units (based on ambient temperature) with species-specific thermal threshold requirements for flowering. Each genus also has an associated pollen production response curve precipitation or both ambient temperature and precipitation. The important physical properties of the pollen representative of each genus such as density, aerodynamic diameter, and average height were used to calculate their deposition velocity.

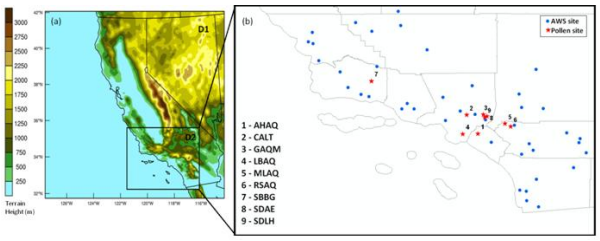

Fig 2. (a) Domain coverage of 12-km California (D1) and 4-km Southern California (D2) with terrain height and (b) the location of pollen sampling sites (red) and the AWS sites (blue)

2.3 NCAR STAMPS model

The magnitude of pollen available for release (potential) in each grid cell for a given species is determined as:

$$\text{Emission} = \varepsilon_{sp} \cdot \alpha_{P,TP} \cdot \gamma$$

where ε_{sp} is the pollen pool size (grains/unit area), which was directly derived from literature values or the associated average values for the PFT that a given species belongs to; $\alpha_{P,TP}$ is a coefficient with values between 0 and 1 that modifies the pool size according to either precipitation (α_P) or both temperature and precipitation (α_{TP}); and γ is the total area occupied by the species. γ was determined using fractional vegetation and land cover datasets such as the National Land Cover Database and species inventories from different sources including Forest Inventory & Analysis

datasets (FIA), Natural Resources Conservation Service datasets (NRCS) and the Cropland Data Layer from National Agricultural Statistic Service (CDL/NASS). STAMPS was run 4 km × 4 km grid cell resolution.

The onset and duration of pollen season for each species was based on the thermal time approach, modeled after García-Mozo et al. (2002). Pollen is available to be released into the atmosphere after a prescribed threshold of heat-accumulation units (i.e., Growing Degree Days, GDD) is achieved. For some species with dual heating and vernalization requirements (e.g., birch, olive, and walnut species), chilling units must also be accumulated until a species-specific chilling threshold has been achieved before GDD accumulation is initiated. The chilling module for olive, walnut and birch tree was based on the chill-heating model of De Melo-Abreu et al. (2004), in which the accumulation of chilling units is determined via a piecewise approximation using the ratio of actual hourly temperature data for a location to an optimal chilling temperature for a given species. After initiation, the distribution of the potential pollen pool is assumed to be log-normal over a two-week duration.

2.4 Pollen emission flux parameterization

Since the STAMPS pollen potential module in MEGAN already explicitly accounts for the daily pollen potential P_a (grains m^{-2}) for different species based on species-specific temperature-precipitation regression mechanisms, only the wind effect in scaling the pollen potential P_a to calculate the rate of emission into the atmosphere was considered. The hourly average vertical emission rate E_P (grains s^{-1} m^{-2}) at each grid cell is proportional to P_a , u_* (m s^{-1}), and wind effect scale factor K_e:

$$E_P = \frac{P_a}{H_s \cdot C} \cdot K_e \cdot u_*$$

where the constant C is the conversion constant from day to seconds, and H_s (m) is the average species-specific canopy height

Wind effect scale factor K_e is a non-dimensional factor with values between 0 and 1 and parameterized following Helbig et al. (2004) using threshold friction velocity u_{*te}, which is a product of resistant factor α and standard threshold friction velocity u_{*t} (m/s):

$$K_e = \begin{cases} 1 - \dfrac{u_{*te}}{u_*}, & u_* > u_{*te} \\ 0, & u_* \le u_{*te} \end{cases}$$

$$u_{*te} = \alpha \cdot u_{*t} = \alpha \cdot \left(0.0123 \times \left[\frac{\rho_P}{\rho} \cdot g \cdot d_p + \frac{0.0003}{\rho \cdot d_P}\right]\right)^{\frac{1}{2}}$$

The form of u_{*t} is the regression formula base on wind tunnel study (Greeley & Iversen, 1985) and related to the pollen density ρ_P (kg/m^3) and aerodynamic diameter d_P (m). ρ is air density (kg/m^3), which is an output of MCIP based the WRF results, and g is gravity acceleration (9.8 m s^{-2}). Resistance factor α is the ratio of an empirical threshold wind speed U_{10e} and the modeled 10-meter wind speed U_{10}:

$$\alpha = U_{10e}/U_{10}$$

The dry deposition process for pollen dispersion is considered in CMAQ by calculating the settling velocity V_{dp} (m/s):

$$V_{dp} = \frac{\rho_p \cdot g \cdot C_c \cdot d_p^2}{18\mu}$$

where C_C is slip correlation coefficient and μ is viscosity of air as a function of temperature.

3. RESULTS AND DISCUSSION

3.1 Meteorological simulation

Simulation of ambient pollen counts needs WRF model to accurately predict meteorological fields, especially the spatial distribution of wind pattern given the complex terrain in Southern California featured with diurnal land-sea breeze and mountain-valley circulation. The comparison of observed and simulated wind rose plot of surface wind during March to June 2010 at two sites is shown in Fig. 3. The UC Riverside site (Fig. 3a) shows that the observed and modeled wind rose patterns are quite similar with nearly 50% occurrence of southerly and 50% northwesterly winds and average wind speed around 3-4 m s^{-1} during the four-month simulation period. The WRF model with the data assimilation technique performed well for wind speed as well as wind direction at this site. For the Pomona site (Fig. 3b), which is several miles away from the Caltech pollen sampling site (CALT, Fig. 2), the model performed less well. Southwesterly wind is the dominant wind direction (more than 90% occurrence). Even though the model matches the observed wind direction, it has the tendency to overestimate wind speed under mild wind conditions.

3.2 Pollen potential and emission rate

Fig. 4 provides spatial distribution of simulated emission potential of six pollen genus during Mar-

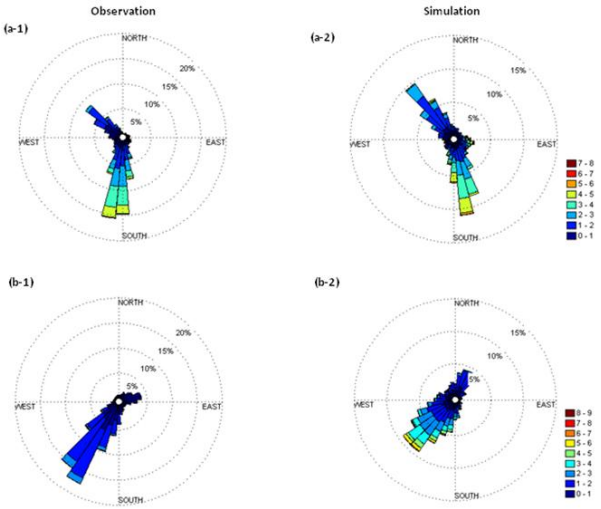

Fig 3. Comparison of observed (left column) and simulated (right column) wind rose plot during March to June 2010 at UC Riverside (33.96ºN, 117.33ºW) (top) and Pomona (34.05ºN, 117.81ºW) (bottom)

Jun 2010 over the 4-km domain (D2). The spatial pattern of different pollen genus varies with birch tree (Fig. 4a), walnuts tree (Fig. 4c), mulberry tree (Fig. 4d) and olive tree (Fig. 4e) mostly populating along the costal place, while the grass (Fig. 4b) and oak tree (Fig. 4f) nearly occupying the whole simulation domain. Notice that the color bar is labeled with logarithmic scale; the variation of estimated emission rate for different grid cells is high. For instance, the variation of oak tree emission potential for different grid cells has ten order of magnitude difference with the maximum value (1.0×10^{18} grains) along southeast border while the minimum value (1.0×10^{8} grains) near upper left corner of the domain. In terms of the total sum of emission potential over the four months simulation time, oak tree has the highest pollen potential with estimated more than 1.0×10^{15} grains over nearly half of grid cells, while the typical value for walnuts trees is only 1.0×10^{9} ~ 1.0×10^{10} grains. The representative of estimated emission rates and locations of each pollen genus will obviously impact the final model performance of simulated pollen concentrations.

By using the pollen emission parameterization scheme described in section 2.4, the hourly gridded emission rates of the six pollen species were calculated for input into the CMAQ model. Only a portion of the pollen potential amount can be emitted into atmosphere due to constrain of wind conditions. Depending on the different pollen genus, the average percent of pollen potential P_a being emitted varied from 5% for oak to 85% for birch under the base case model configuration.

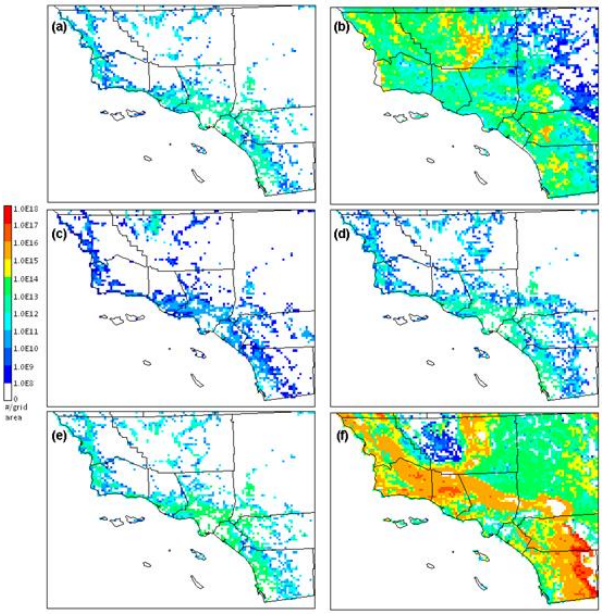

Fig 4. Simulated spatial pattern of emission potential during Mar-Jun 2010 for (a) birch tree, (b) grass, (c) walnuts, (d) mulberry, (e) olive, and (f) oak.

3.3 Pollen concentration

Fig. 5 provides the time series comparison of six simulated pollen genus during the four-month simulation window at the Caltech site (CALT). For birch tree (Fig. 5a), the model can reproduce the peak in early May but miss the earlier observed peaks during March. This is expected due the lack of temporal alignment between modeled pollen season and observed concentrations at large scale. The model has poor performance for bromus grass at the CALT site in terms of both the mean value (overestimation by the factor of 6) and daily variation trend (Fig. 5b). For walnut tree (Fig. 5c), the simulated concentration is very sparse and systematically low (1 grains m^{-3}) compared to observed values, which suggests the pollen potential may be underestimated. The vegetation datasets used in this study may have significantly underestimated walnut distribution by mis-counting the large portion of home-owned walnuts tree at suburban community over southern California (Duhl et al., 2012). The simulations for mulberry (Figure 5d) and olive tree (Fig. 5e) at CALT are reasonably good in terms of following the daily variation trend and keeping the ratio between simulated and observed mean within a factor of 2. In contrast, the current modeling configuration for oak tree performs less at the Caltech site (Fig. 5f).

Table1 documents the comparison between observed (OBS) and corresponding simulated daily mean of pollen genera concentrations (grains/m^3) for this set of model configuration

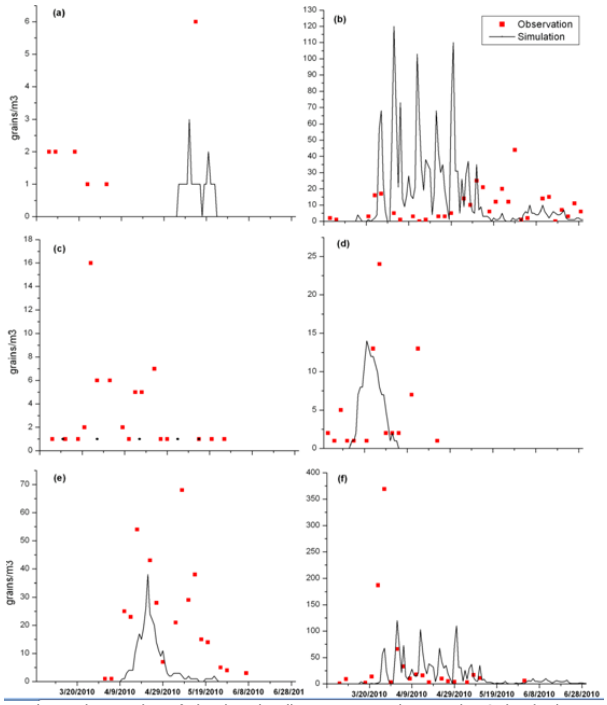

Fig 5. Time series of simulated pollen concentrations at the Caltech site (CALT) during Mar-Jun 2010 for (a) birch tree, (b) grass, (c) walnuts, (d) mulberry, (e) olive, and (f) oak.

(case code 'BASE'). The model performance for birch, olive and mulberry pollen are reasonable good with bias less than ±100%. The base case configuration tends to overestimate the mean grass pollen concentration 4~5 times especially at the north Santa Barbara and south Riverside region. Grass pollen is widely spread over the southern California simulation domain (Fig 4b). The representative of emission factor and the land cover database used to allocate the emission is the important to the concentration simulation. The model also tends to underestimate the walnuts concentration, the simulated mean at each region is less than 1 grains/m^3. The walnuts emission potential is small during the simulation window comparing with other pollen genera, hence the observation level is also low. The emission module also miss-counts the substantial home-owned backyard walnuts tree for the suburban at Los Angeles region.

3.4 Sensitivity of boundary conditions, emission pool and friction velocity to pollen concentration

The sensitivity runs of pollen simulation by using dynamic boundary conditions from domain D1 CMAQ simulation (case code 'BCON'), by taking the upper (case code 'PAHI') and lower (case code 'PALO') estimates of pool size for each pollen genus, and by varying the value of empirical threshold wind speed the value of U_{10e} to 2.0 m/s (case code 'UTLO') and 4.0 m/s (case code 'UTHI') were conducted with the results shown in Table 1 also. Considering dynamic boundary conditions may slightly improve simulated value near the boundary especially for grass and oak pollen. Compared with case run 'BASE', the variation of pollen production size pool can impact the final simulation results by 30% or more. Case run 'PALO' for walnut pollen simulation agrees better with observation means, which implies the tendency of emission underestimates over most of the domain. However, the WRF-CMAQ model still systematically overestimates grass and oak pollen concentration at north region and underestimates oak pollen concentration for the rest part of domain, which implies the possible deficit of pollen emission spatial allocation or the pollen release parameterization scheme. No obvious model improvement was found for case run 'UTLO' and 'UTHI' compared with base case.

Table 1. Evaluation of simulated daily mean of pollen species concentration (grains/m^3) for different cases over southern California

		Mean (grains/m^3)					
	OBS*	BASE*	BCON*	PAHI*	PALO*	UTHI*	UTLO*
Santa Barbara(1)							
Birch	0	0	0	0	0	0	0
Grass	8	34	36	42	27	32	35
Walnuts	0	1	1	2	1	1	1
Mulberry	0	0	0	1	0	0	0
Olive	2	3	3	4	2	3	3
Oak	4	22	27	32	13	23	25
LA Metropolitan Area(2)							
Birch	1	0	0	0	0	0	0
Grass	10	6	7	19	4	6	6
Walnuts	1	0	0	1	0	0	0
Mulberry	3	2	2	2	2	2	2
Olive	6	3	3	5	2	3	3
Oak	11	7	8	13	4	6	8
Riverside & Orange(3)							
Birch	1	1	1	1	1	1	1
Grass	5	31	31	43	19	28	34
Walnuts	2	0	0	1	0	0	0
Mulberry	4	1	1	2	1	1	1
Olive	3	2	2	3	2	2	2
Oak	29	10	10	16	8	9	10

*OBS – observations; BASE – base case; BCON – case study with pollen concentration influenced by outside simulation; PAHI – sensitivity study with upper bound of pollen pool estimates (equation 2); PALO – sensitivity study with lower bound of pollen pool estimates; UTHI – sensitivity study with lower threshold friction velocity (equation 3) ; UTLO – sensitivity study with lower threshold friction velocity.
(1) Santa Barbara: includes pollen count sites 'SBBG' (Figure 2); (2) LA Metropolitan Area: includes pollen count sites 'CALT', 'LBAQ', 'GAQM', 'SDAE' and 'SDLH'; (3) Riverside & Orange: includes pollen count sites 'AHAQ','MLAQ' and 'RSAQ'.

4. SUMMARY

Exposure to bioaerosol allergens such as pollen can trigger allergenic airway disease (AAD) in a significant portion of sensitive populations and thus can cause serious public health problems. Assessment these health impacts by linking the airborne pollen levels, concentrations of respirable allergenic material, and human allergenic response under current conditions and being able to make predictions about how these impacts might change in future climate conditions is a key step toward developing preventive actions. To that

end, a regional-scale pollen emission and transport modeling framework was developed that treats allergenic pollens as non-reactive tracers within the WRF/CMAQ air-quality modeling system. The STAMPS model was developed to generate daily a pollen pool which can then be emitted into the atmosphere by wind. It is driven by species-specific meteorological (temperature and/or precipitation) threshold conditions and is designed to be flexible with respect to its representation of vegetation species and plant functional types (PFTs). The hourly pollen emission flux was parameterized by considering pollen pool, friction velocity, and wind threshold values. The dry deposition velocity of each species of pollen was estimated based on pollen grain size and density. The evaluation of pollen modeling framework was conducted over southern California during March to June 2010. This period coincided with observations by the University of Southern California's Children's Health Study (CHS), which included O_3, $PM_{2.5}$, and pollen count, as well as sensitization data at nine sites. Two nesting domains with horizontal resolution 12 km and 4 km were constructed and six representative allergenic pollen genera were included: birch tree, walnut tree, mulberry tree, olive tree, oak tree, and grasses. Under current parameterization scheme, the modeling framework tends to underestimate walnuts and peaks in oak pollen concentrations and overestimate grass pollen concentrations, but showed reasonable agreement with observed birch, olive and mulberry pollen concentrations. Sensitivity studies suggested that the estimation of pollen pool is a major source of uncertainty for simulated pollen concentrations. Achieving agreement between emission modeling and observed pattern of pollen releases is the key for successful pollen concentration simulations.

Acknowledgement

This work was supported by US EPA Grant R834358.

References

De Melo-Abreu, J.P., Barranco, D., Cordeiro, A.M., Tous, J., Rogado, B.M., Villalobos, F.J.: Modelling ovlive flowering data using chilling for dormancy release and thermal time, *Agricultural and Forest Meteorology*, 125, 117-127, 2004.

García-Mozo, H., Galán, C., Aira, M.J., Belmonte, J., Diáz de la Guardia, C., Fernández, D., Gutierrez, A.M., Rodriguez, F. J., Trigo, M.M., and Domingues-Vilches, E.: Modeling start of pollen season in different cliantic zones in Spain, *Agricultural and Forest Meteorology*, 110, 247-257, 2002.

Greely, R., and Iversen, J.D.: Wind as a geological process on Earth, Mars, Venus and Titan, Cambridge University Press, New York, 1985.

Helbig, N., Vogel, B., Vogel, H., and Fiedler, F.: Numerical modeling of pollen dispersion on the regional scale, *Aerobiologia*, 3, 3-19, 2004.